

TWO APPROACHES IN SCANNER-PRINTER CALIBRATION: COLORIMETRIC SPACE-BASED VS. "CLOSED-LOOP".

V. Ostromoukhov, R.D. Hersch, C. Péraire, P. Emmel, I. Amidror

Swiss Federal Institute of Technology (EPFL)
CH-1015 Lausanne, Switzerland.

Abstract

The present paper studies two different table-based approaches for the calibration of electronic imaging systems. The first approach, which is the classical one, uses the device-independent CIE-XYZ colorimetric space as an intermediate standard space. Input and output devices such as scanners, displays and printers are calibrated separately with respect to the objective CIE-XYZ space. The calibration process requires establishing a 3-dimensional mapping between a scanner's device-dependent RGB space and a device-independent colorimetric space such as CIE-XYZ. Measured samples belonging to the calibration set are used for splitting the colorimetric space into Delaunay tetrahedrons. The second approach, the so-called *closed loop* approach, calibrates directly scanner-printer pairs, without any reference to an objective colorimetric space. It enables a 3-D mapping to be built between the scanner's RGB space and the printer's CMY space without requiring any colorimetric measurement. It offers very accurate calibrated output for input samples having the same characteristics (halftone dot, ink spectral reflectance) as the printed samples used for the calibration process. When the desktop scanners' RGB sensibilities are not a linear transform of the CIE \bar{x} , \bar{y} , \bar{z} matching curves, an accurate calibration can only be made if input color patches are based on the same primary inks as the patches used for device calibration.

1. Introduction

Due to the increase in available processing power and memory space, table-based calibration seems to offer efficient solutions for the calibration of desktop input/output color devices such as scanners and printers.

Previous work has been related either to the theoretical analysis of 3-D table-based calibration methods [Hung93] or to the calibration of particular output devices [Nin92]. The present work aims at comparing two approaches for the calibration of color input/output devices. In the first approach, we try to calibrate input devices separately by establishing a 3-dimensional mapping between a scanner's device-dependent RGB space and a device-independent colorimetric space such as CIE-XYZ or CIE-LAB and a 3-D mapping between the chosen device-independent colorimetric space and a given printer's CMY output space. The considered 3-D non-linear mappings are based on the segmentation of the colorimetric input spaces into Delaunay tetrahedrons whose vertices are given by elements of the calibration set. For each new RGB sample, tri-linear interpolation within the corresponding tetrahedron is applied, first in the RGB space in order to obtain its XYZ values, and then in the CIE-XYZ space in order to obtain its CMY values. This solution provides continuity at the boundaries of the Delaunay tetrahedrons and offers a predictable result within the printer's gamut.

In the second approach, the *closed loop* or *scan-back* approach, we establish a direct 3-D relationship between the input device RGB space and the output device CMY space. Printed samples generated on the target output device with known output device coordinates are directly scanned, thus enabling the characterization of the scanner's input space with respect to the printer's output space.

In this work, device calibration methods are applied to a real desktop scanner-printer pair. Desktop devices are far from being perfect: we will show that position and neighborhood affect the scanned pixel values and that the

scanner's RGB sensitivities are not linear transforms of the CIE \bar{x} , \bar{y} , \bar{z} matching curves. Special care is therefore required to minimize these undesirable effects.

The calibration process maps a 3-D device-dependent input space into a 3-D device-dependent output space. If the printer driver uses a continuous undercolor removal (UCR) and gray component replacement (GCR) strategy, UCR and GCR can be considered to be part of the non-linear printer behavior. Therefore, the proposed approach can also be used for CMYK printing.

2. Characterization of desktop scanners

A study of the characteristics of a typical flatbed desktop scanner (Agfa Arcus Plus) demonstrated a number of imperfections. We have identified (1) scanning window boundary effects, (2) R,G,B sensibilities which are not a linear transformation of the \bar{x} , \bar{y} , \bar{z} matching curves, and (3) a significant influence of the neighborhood on a scanned pixel value.

Boundary effects

The digitization of uniformly colored samples covering the whole scanner window shows boundary effects. The deviation between the color coordinates of a sample point scanned at the center of the window, and those of a sample point scanned at the scanner's window boundary reaches $\Delta E = 5.0$ (CIELAB). These boundary effects can be reduced by scanning only in the central part of the scanner's window (Fig. 2.1).

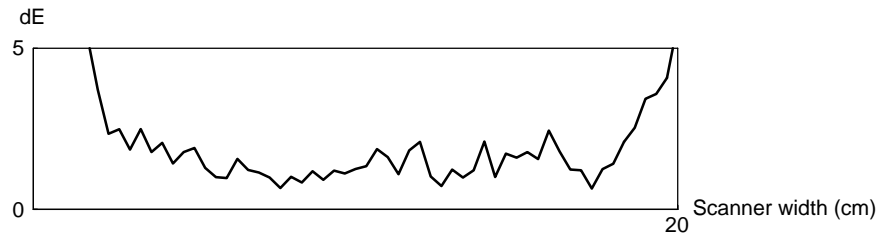


Fig 2.1. Location-dependent scanning errors

Unsuitable scanner R,G,B sensibilities

Experiments on desktop scanners have shown that color patches produced with different inks having identical LAB coordinates may generate quite different R, G, B values. Moreover, patches which produce identical scanned R, G, B values may differ by more than $\Delta E = 10$ in CIELAB. Generally, desktop color scanner sensitivities are not a simple linear transformation of the sensitivities of the human eye's cones, which are expressed indirectly by the CIE \bar{x} , \bar{y} , \bar{z} matching curves [Farell93]. This explains why colors which are seem identical to the human eye do not appear identical for the scanner and vice-versa. Input devices having such properties are referred to as "non-colorimetric" scanners.

Neighborhood influence on scanned pixel values

In order to analyze the influence of the neighborhood upon scanned pixel values, we scanned a horizontally or vertically oriented half-white half-black sample sheet. The sharp white-black transition occurs at position 0. Figure 2.2 illustrates the *achromatic* influence of the neighborhood on the scanned pixel values. In the vertical direction a neighborhood of ± 1 centimeter influences the scanned pixel value. In the horizontal direction, a neighborhood of ± 3 to ± 4 cm influences the scanned pixel value. The higher influence of the horizontal neighborhood is due to the fact that a horizontally oriented wide and thin light source scans the sample sheet in parallel with the CCD sensor. The influence of the neighborhood is therefore more significant horizontally than vertically.

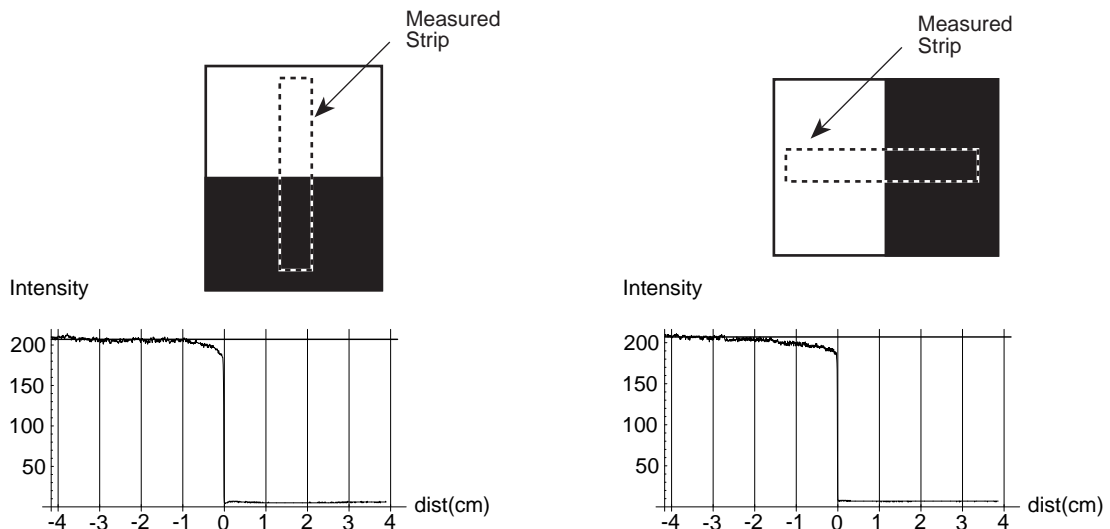


Fig. 2.2. Achromatic influence of vertical and horizontal neighborhoods

A further experiment analyzes the *chromatic* influence of the neighborhood in the horizontal direction. For this purpose a 5mm wide constant 50% gray strip is surrounded by colors varying either along the black-white or along the red-cyan diagonal of the CMY output device cube (Fig. 2.3b). In Fig. 2.3c, the large dot indicates the RGB coordinates of the constant gray strip; the origins of the arrows are the scanned RGB values of the neighborhood at the selected locations of the considered CMY cube diagonal. Each colour difference vector plotted in Fig 2.3c expresses the scanned difference between the gray patch surrounded by its own gray value and the gray patch surrounded by the selected neighborhood colour. These difference vectors are scaled by a factor of 3 in order to enhance their visibility.

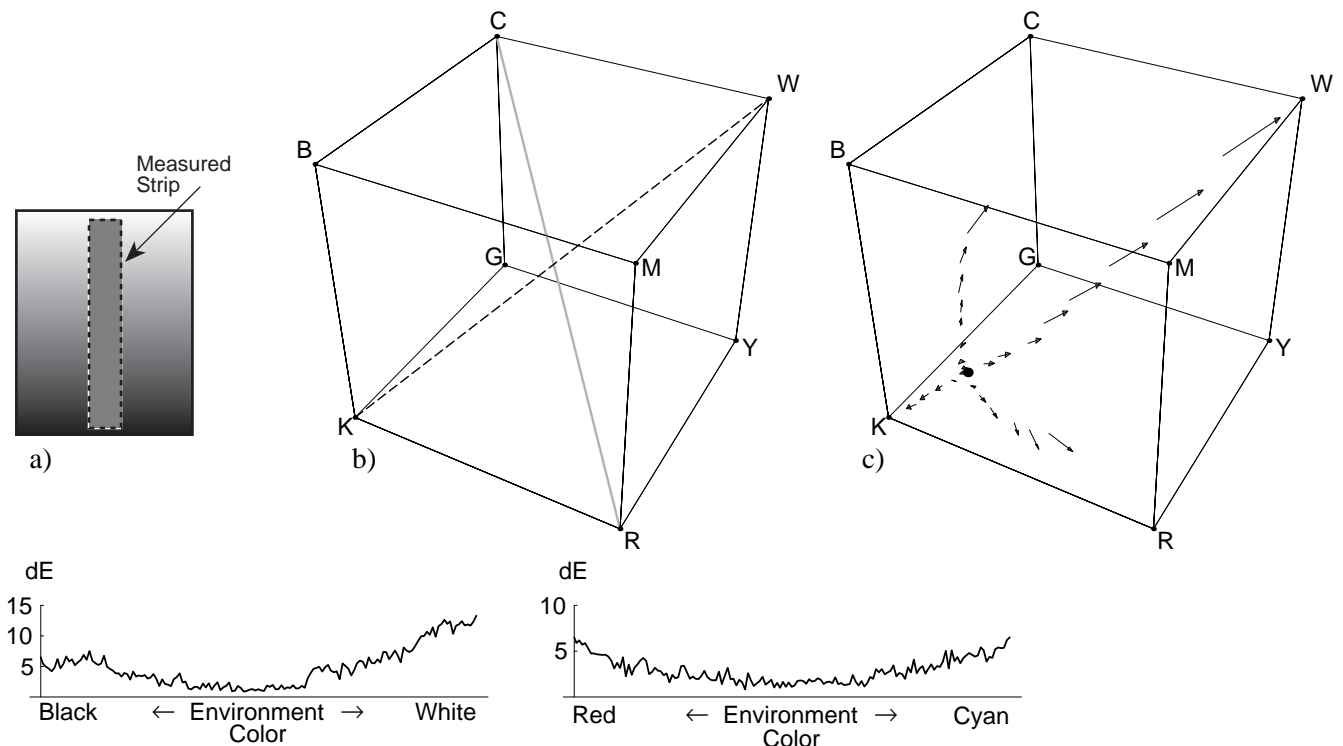


Fig. 2.3. Chromatic influence of horizontal neighborhoods

It has been found that the chromatic neighborhood influence has the effect of pulling the constant gray point towards the color of its neighborhood, in a similar way as the intensity of an achromatic sample is influenced by its neighborhood (see Fig. 2.3c).

3. Separate calibration of input and output devices by tetrahedral interpolation

Input devices can be characterized by the device-dependent RGB and device-independent XYZ coordinates of sample colors belonging to the input calibration set. Output devices are characterized by the device-independent XYZ coordinates and the CMY device-dependent printable values of sample colors belonging to the output calibration set. Points of the calibration set should be well distributed within the reproducible gamut. The calibration procedure requires the tetrahedrization of both the volumic RGB input space and the volumic CIE-XYZ output space with their respective sets of calibration samples. Thanks to the tetrahedrization of the input calibration set in the RGB space, the RGB→XYZ colour space transformation required for calibrated scanning can be performed. Tetrahedrization of the output calibration set in the CIE-XYZ space must be performed before the XYZ→CMY colour space transformation required for calibrated printing. At scanning time, the XYZ value of a new RGB sample is interpolated from the 4 samples of the calibration set which form the vertices of the tetrahedron enclosing the new RGB value. Similarly, the CMY value of a new XYZ sample to be printed is interpolated from the 4 samples of the calibration set which form the vertices of the tetrahedron enclosing the new XYZ value.

The sample colors belonging to the calibration set form a set of points either in the RGB space for input device calibration or in the CIE-XYZ space for output device calibration. The volume spanned by these points must be decomposed into tetrahedrons. There is an infinity of possible decompositions. We have chosen the Delaunay tetrahedrization. The fundamental property of this tetrahedrization is that no point of the calibration set belongs to the interior of the spheres circumscribing the tetrahedrons. The Delaunay tetrahedrization is the only tetrahedrization with that property [Boissonat86]. In practice, it implies that, in the general case, the tetrahedrons are neither "too flat" nor "too long". Therefore, the volume on which the interpolation will be performed has a reasonable shape. The Delaunay tetrahedrization is calculated by Watson's algorithm [Watson81] with a complexity of $O(N^2)$.

Calibrated scanning or printing requires finding to which tetrahedron a new point M belongs. The procedure works as follows: Let I be a point belonging to a known tetrahedron T . M belongs to the same tetrahedron if there is no intersection between segment IM and any surface of T . In this case we have found the tetrahedron to which M belongs. If an intersection with one of the tetrahedron's surfaces exists, a new point I is chosen in the tetrahedron adjacent to T , which shares with T its intersected surface. The procedure is repeated until the correct tetrahedron is found. In theory, the complexity of this procedure is $O(N^2)$. But if the points of the calibration set are uniformly distributed, the number of tetrahedrons is only $O(N)$ [Boissonat86] and the desired tetrahedron can be found with a computational effort proportional to $N^{1/3}$. Using 949 Pantone color samples as the calibration set, we obtain a fairly uniform tetrahedral decomposition with a mean ratio of 4 to 5 tetrahedrons per sample point.

Tetrahedron search can be made much faster by decomposing the considered 3-D space into cubic cells, for example into $16 \times 16 \times 16$ cells. Each cell contains a list of tetrahedrons intersecting the cell. Once the cell enclosing target point M is found, the procedure described above is applied to select the correct tetrahedron among the candidate tetrahedrons intersecting the cell.

As shown in the previous section, calibration of desktop scanners is, due to neighborhood effects and non-colorimetric RGB sensitivities, much more critical than calibration of desktop printers. Let us therefore describe first the output calibration procedure based on experiments made with the desktop color printer HP DeskJet 1200C/PS.

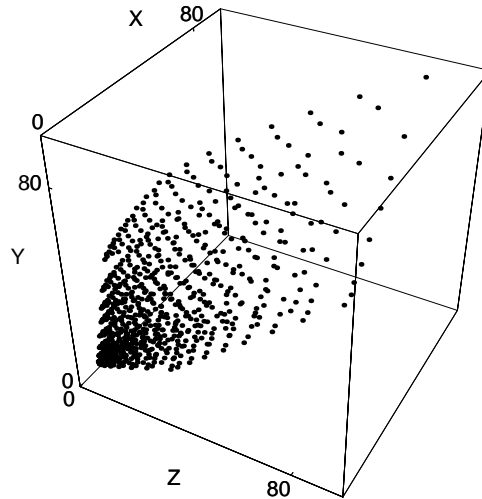


Fig 3.1. Gamut of the calibration set used for calibrating the printer in the CIE-XYZ space

Output device calibration

In order to calibrate an output device printing with 3 basic inks (Cyan, Magenta, Yellow), we first generate a set of 9x9x9 color CMY equally-spaced patches forming the calibration set. The device-independent CIE-XYZ or CIE-LAB colorimetric values of these patches are measured with a spectrophotometer (Gretag SPM 100). This calibration set defines a 3-D mapping between color independent CIE-XYZ or CIE-LAB space to the CMY output device space. Figure 3.1 shows the distribution of the calibration set in the CIE-XYZ space.

The same tetrahedrization algorithm as described above is applied in order to segment into tetrahedrons the printer's volumic gamut given by this calibration set of 9x9x9 printed samples. The testing set consists of new points with given XYZ coordinates formed by those colour samples of the Pantone catalog which are inside the gamut of the printer.

The quality of this output device calibration process is analyzed by computing CMY values for the samples of the testing set. For each sample, the corresponding tetrahedron in the device-independent space (XYZ or LAB) is found and CMY values are obtained by linear interpolation between the samples of the calibration set determining the tetrahedron's vertices. Then, the resulting CMY color is printed and compared with the original Pantone color.

Analyzing the results, the following problematic cases were found:

- a) If the calibration set forms a non-convex volume in the CIE-XYZ or CIE-LAB spaces, the tetrahedrization may produce inadequate tetrahedrons at the volume's concavities. These tetrahedrons are easily detected: their corresponding tetrahedrons in the CMY space are completely flat and located at the gamut's boundary. Such degenerated tetrahedrons need to be removed.
- b) Tetrahedrons defined by vertices lying on different sides of the gray axis may be responsible for considerable errors. The probability of having large tetrahedrons crossing the gray axis can be diminished by densely populating areas close to the gray axis in the calibration set.
- c) The colorimetric value of printing inks from successive cartridges was found to vary considerably. Variations may be due to the current ink volume in the cartridge, to ink utilization rate and to other environment parameters (temperature, humidity).

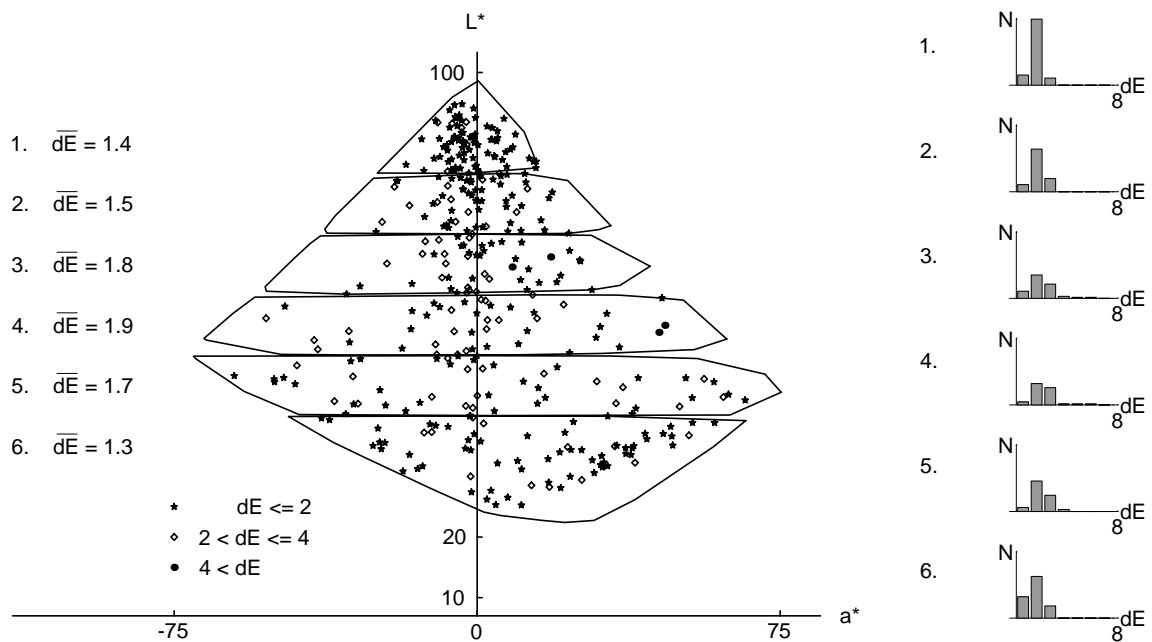


Fig 3.2. Errors between predicted and measured output values (mean error $\overline{\Delta E} = 1.6$, standard deviation $\sigma = 0.7$)

The results shown in Fig. 3.2 were obtained after eliminating the calibration set samples responsible for concavities (case a) and retriangulating the XYZ volume. Gamut mapping was not considered and test samples lying outside the printable gamut were eliminated. The calibration set was not more densely populated along the gray axis as proposed above (case b). The difference between predicted and measured values is expressed in ΔE units relative to the CIE-LAB space (Fig. 3.2). Mean errors and the error distributions are given for the different luminance slices (L^*).

Input device calibration

As mentioned in section 2, limitations of present desktop scanners require special care for accurate calibration. Color patches should be sufficiently large to avoid neighborhood effects. Due to the scanner's non-colorimetric RGB sensitivities, the patches belonging to the calibration set should be based on the same primary inks as the patches used for the tests.

In the experiments we carried out for separate input device calibration, the conditions for accurate calibration could not be fulfilled. The calibration set is formed by the small patches of the Pantone catalogue. The testing set is formed by 128 small patches of the ColorCurve catalogue whose spectral reflectance is quite distant from that of Pantone colors.

Fig. 3.3 shows the mean-error at different levels of the luminance axis (L^*).

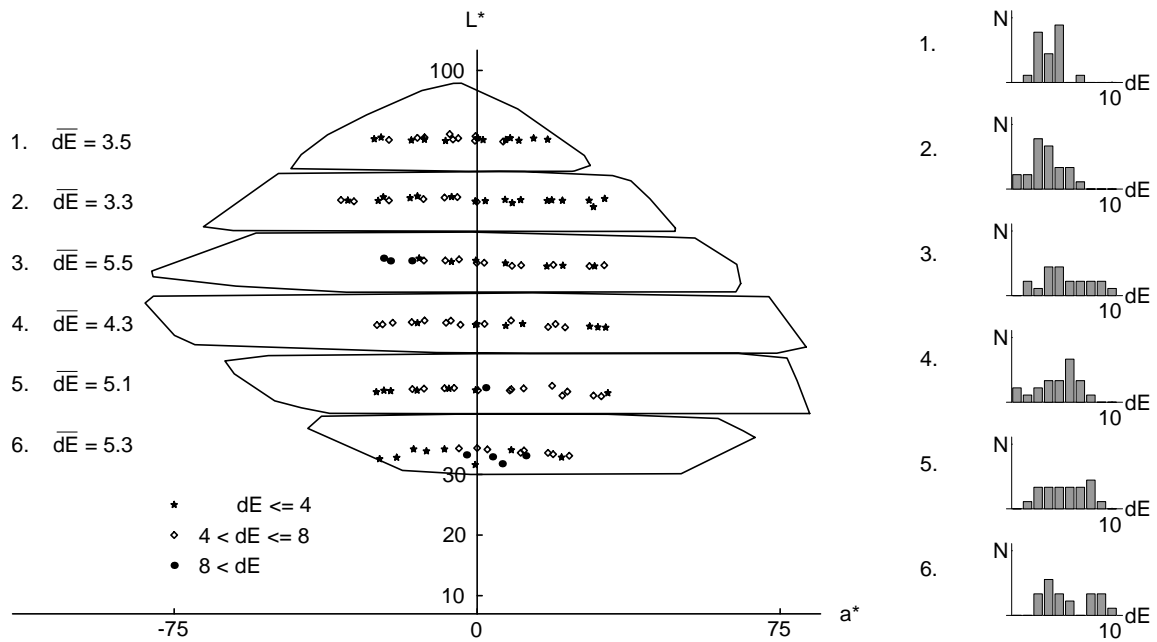


Fig 3.3. Errors between the predicted and the measured XYZ value of scanned samples, expressed in terms of CIELAB ΔE differences (mean error $\overline{\Delta E} = 4.5$, standard deviation $\sigma = 2.2$)

Combined input-output calibration

Let us now consider the results obtained from combined table-based calibration of both input and output values. The XYZ value of each scanned sample is obtained by finding the corresponding tetrahedron in the RGB \rightarrow XYZ transformation space and interpolating between the XYZ values of the tetrahedron's vertices. Corresponding printable CMY intensities are obtained by the same procedure, applied to the XYZ \rightarrow CMY transformation space.

Figure 3.4 shows the accuracy of the combined calibrated scanning and printing process. The overall average error is $\Delta E = 5.5$.

Due to the imperfect behavior of the desktop scanner and, to a smaller extent, of the printer, calibration by interpolation in Delaunay tetrahedrons gives only approximative results which may however be sufficient for limited quality desktop reproduction. These results can be improved by (a) densifying the number of sample points belonging to the calibration set around the gray axis, (b) calibrating the scanner with color patches of size 8cm x 2cm, and scanning only their center in order to avoid neighborhood effects and, (c) when calibrating color, using patches based on the same primary inks as the patches used for the tests.

This method, used in conjunction with a higher-quality scanner, offers the following major advantages: The Delaunay tetrahedrization can be performed on any set of samples as calibration set. Each input or output device (scanner, printer, display...) is independently calibrated with respect to a reference space (CIE-XYZ or CIE-LAB). Calibrated scanning and printing devices can therefore be assembled freely.

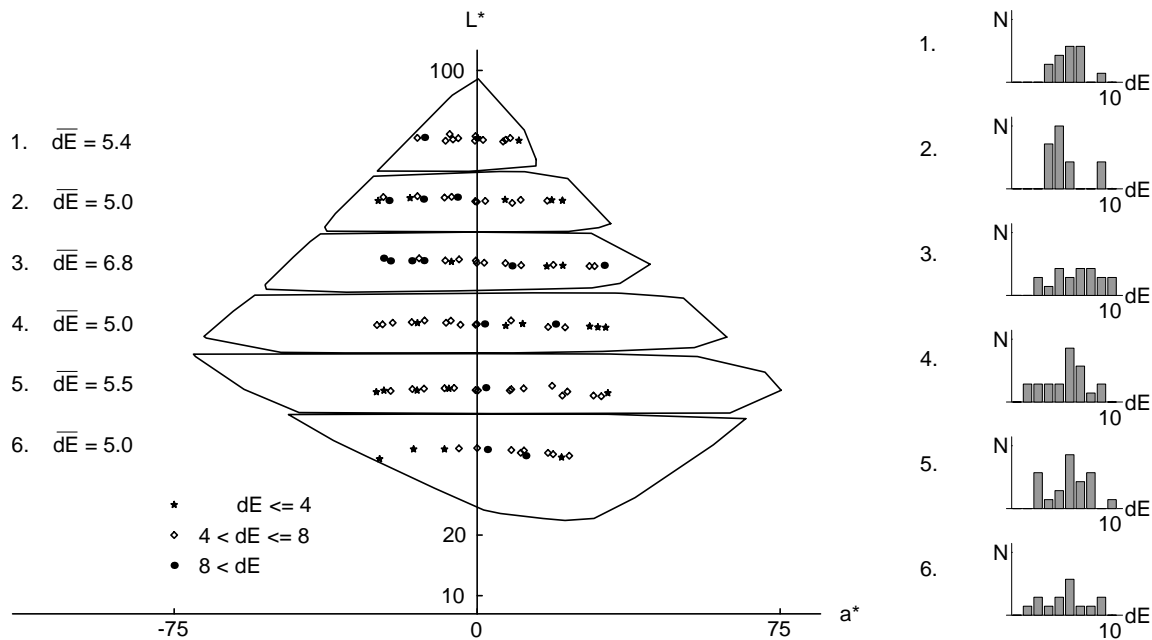


Fig. 3.4. Errors between measured input and output values for the full color reproduction process (mean error $\Delta E = 5.5$, standard deviation $\sigma = 2.1$)

4. The closed loop approach

In the closed loop approach, we simultaneously calibrate a scanner-printer pair by establishing a direct 3-D relationship between the input device's RGB space and the output device's CMY space. A calibration set of known CMY equally spaced 9x9x9 printed samples is generated on the target printer. These samples have a width of 8cm and a height of 2 cm so as to avoid the neighborhood interferences described in section 2.

These samples are directly scanned, thus enabling the characterization of the scanner's input space with respect to the printer's output space. This process enables building a 3-D RGB space containing points with known CMY values. In the CMY space, points belonging to the calibration set are the vertices of a 3-D cubic grid. Each cube in this grid is decomposed into 6 tetrahedrons [Hung93]. The same decomposition is applied to corresponding points in the RGB space. The so-obtained tetrahedrons are used for interpolating new CMY values from known RGB values of scanned color pixels.

This closed loop approach also works with CMYK printers. With CMYK printers, we assume that an intermediate CMY description is used to feed the undercolor removal function. If undercolor removal is a continuous function, it can be considered to be part of the non-linear printer behavior. Therefore, the mapping between the RGB and CMY space described above can be used to produce the CMY color coordinates feeding the undercolor removal process which produces the C'M'Y'K' color separation values. Since the printed samples belonging to the calibration set incorporate black as one their basic inks, black is implicitly present in the calibration process.

The closed-loop method produces the best results so far: With a testing set of 128 samples, we obtain for samples within the printable gamut a mean error between input and output values of $\Delta E = 2.37$, with a standard deviation $\sigma = 1.26$. Figure 4.1 shows the distribution of the errors for the different luminance levels.

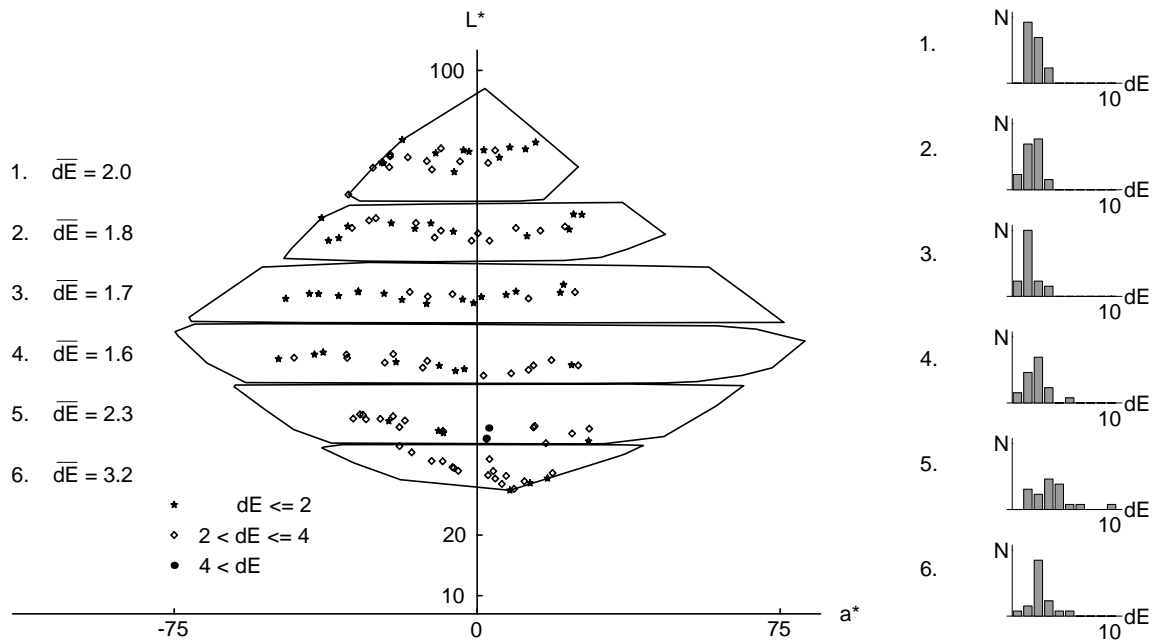


Fig. 4.1. Errors between measured input and output values for the full closed loop color reproduction process (mean error $\overline{\Delta E} = 2.37$, standard deviation $\sigma = 1.26$)

The closed-loop approach shows that with desktop equipment 3-D mapping can provide highest quality results when input test samples have the same properties as samples of the calibration set printed by the target printer (same paper, same spectral characteristics of the primary inks, same halftoning technique). When these conditions are fulfilled, inaccuracies of the scanning device are integrated into the 3-D non-linear mapping. This mapping provides for the scanned test samples precise predictions of the CMY values to be printed.

5. Conclusions

We have presented two approaches for the table-based calibration of desktop scanning and printing devices. The first approach consists in a separate mapping of RGB input values to XYZ device-independent values and of XYZ values to CMY output device coordinates. The second approach consists in mapping RGB input values directly to output device CMY values.

The first approach allows the separate calibration of input and output devices. However, it requires measuring the XYZ values of the patches forming the calibration set for both input mapping and output mapping. Furthermore, at image rendering time, two 3-D table-based accesses and interpolations are necessary to compute CMY output device coordinates from RGB scanned pixel values. Since tedious measuring work is necessary for each calibration, it is not easy to re-calibrate a device in order to obtain higher accuracy for new input data such as a finer halftone algorithm, or a higher quality paper.

In the second approach, an input-output device pair is calibrated by a single 3-D table. Since the values of the printed patches belonging to the calibration set are known, there is no need for tedious spectral measurements. The printed values are fed to the scanner in order to obtain the RGB coordinates corresponding to the CMY values of the printed patches. Since this input-output device pair calibration is done for the specific reproduction process used by the printer (for example, for a given halftoning algorithm), it produces high-quality results for images reproduced with the same process. Most of the scanner's inaccuracies are included in this closed-loop mapping approach and therefore do not have a negative influence on the results.

Neighborhood influence during the scanner calibration process can be reduced by scanning sufficiently large color patches (calibration set). At reproduction time, accurate output values are predicted for surfaces with smooth

colorimetric variations. Textured surfaces having high colorimetric variations or high-contrast edges are not rendered as accurately as smooth surfaces, but the error is less perceptible than if it would appear on smooth surfaces.

Currently, the closed-loop approach works with high accuracy only for reproducing originals printed with the target printer. In order to become a general-purpose calibration method, scanners should be used which provide (a) colorimetric RGB spectral sensitivities, (b) neighborhood independent scanning and (c) a true low-resolution scanning mode enabling integration over local color variations due to the halftone process.

Acknowledgement

The results for separate input device calibration have been obtained in the framework of the CEE Brite-Euram HIDIPOP project. The remaining parts of the research are financed by EPFL and by the Swiss National Fund (grant No. 21-31136.91).

References

- [Boissonat86] Boissonnat, J.D., "An hierarchical representation of objects: the Delaunay tree", *Proceedings of the 2nd ACM symposium on computational geometry*, Yorktown Heights, June 1986, 260-268.
- [Farell93] J. Farell, B. Wandell, "Scanner linearity", *Journal of Electronic Imaging*, Vol 2, No 3, July 1993, 225-230.
- [Hung93] P.C. Hung, "Colorimetric calibration in electronic imaging devices using a look-up table model and interpolations", *Journal of Electronic Imaging*, Vol. 2, No. 1, January 1993, 53-61.
- [Nin92] S.I. Nin, J.M. Kasson, W. Plouffe, "Printing CIELAB images on a CMYK printer using tri-linear interpolation", *Colour Hardcopy and Graphic Arts*, SPIE Vol. 1670, 1992, 316-324.
- [Watson81] Watson, D.F., "Computing the n-dimensional Delaunay tessellation with application to Voronoi polytopes", *The Computer Journal*, Vol 24, No 2, 1981, 167-172.